Fast isolation of sub-nanomolar affinity alpaca nanobody against the Spike RBD of SARS-CoV-2 by combining bacterial display and a simple single-step density gradient selection

Guillermo Valenzuela Nieto[1], Ronald Jara[1 & 2], Johanna Himelreichs[1], Constanza Salinas[1], Teresa Pinto[1], Yorka Cheuquemilla[1], Yago Margolles[3], Natalia López González del Rey[4], Zaray Miranda-Chacon[1], Alexei Cuevas[1], Anne Berking[5], Camila Deride[1 & 8], Sebastián González-Moraga[1], Héctor Mancilla[1], Daniel Maturana[6], Andreas Langer[6], Juan Pablo Toledo[1], Ananda Müller[7 & 8], Benjamín Uberti[8], Paola Krall[1 & 9], Pamela Ehrenfeld [10 & 14], Javier Blesa[4], Pedro Chana-Cuevas[11], German Rehren[12], Luis Ángel Fernandez[3] & Alejandro Rojas-Fernandez[1, 5,13 & 14]

1 Institute of Medicine, Faculty of Medicine, Universidad Austral de Chile, Valdivia, Chile.

2 Institute of Biochemistry and Microbiology, Faculty of Sciences, Universidad Austral de Chile, Valdivia, Chile.

3 Department of Microbial Biotechnology, National Biotechnology Center, Superior Council of Scientific Research, Madrid, Spain.

4 Comprehensive Neuroscience Center AC (CINAC), HM Puerta del Sur, Madrid Mostoles Hospital, 28938 Madrid, Spain.

5 Berking Biotechnology, Valdivia, Chile.

6 NanoTemper Technologies GmbH, Floessergasse 4, 81369 Munich, Germany.

7 Ross University School of Veterinary Medicine, Saint Kitts and Nevis, West Indies.

8 Institute of Veterinary Clinical Sciences, Faculty of Veterinary Sciences, Universidad Austral de Chile, Valdivia, Chile.

9 Department of Pediatrics and Children's Surgery Oriente, Universidad de Chile.

10 Institute of Anatomy, Histology, and Pathology, Faculty of Medicine, Universidad Austral de Chile.

11 CETRAM & Faculty of Medical Science Universidad de Santiago de Chile, Chile.

12 Technology Transfer and Licensing division, Universidad Austral de Chile, Valdivia, Chile.

13 Center for Interdisciplinary Studies on the Nervous System, CISNE, Universidad Austral de Chile, Valdivia, Chile.

14 Institute of Philosophy and Complexity Sciences, Santiago, Chile.

* Correspondence should be addressed to alejandro.rojas@uach.cl

Abstract

Despite the worldwide efforts to avoid disease progression of COVID-19 into a severe acute respiratory syndrome and avoid its severe impact on health systems; the situation remains critical. Effective diagnosis, treatment, and prophylactic measures are required to meet the worldwide demand: recombinant antibodies such as alpaca Nanobodies fulfill these requirements. Here, we develop a fast track for nanobody isolation against the receptor-binding-domain (RBD) SARS-CoV-2 Spike protein following an optimized immunization, efficient construction of the VHH library for *E. coli* surface display, and single-step selection of high-affinity nanobodies using a simple density gradient centrifugation of the bacterial library. Following this procedure, we isolate and characterize an alpaca Nanobody against Spike RBD of SARS-CoV-2 in the sub-nanomolar range.

Introduction

Coronavirus disease 2019 (COVID-19) is the name given by the World Health Organization to the illness caused by SARS-CoV-2 infection, a novel coronavirus identified in China that is related to pneumonia and multiple organ dysfunction, constituting an unprecedented threat to health and economy worldwide (1-4). Currently, there are no vaccines or drugs that can effectively contain the pandemic, and to flatten the curve and avoid the collapse of health systems, non-pharmacologic public health measures such as social distancing, border closures, and lockdowns have been enforced globally (5, 6). Genetic studies determined that the pathogen responsible for

this outbreak belongs to the Coronaviridae family, genus *Beta-coronavirus*, sub-genus *sarbecovirus (7)*. It has high sequence homology with the bat coronavirus RaTG13, providing evidence that the new virus may have originated in bats (8).

The SARS-CoV-2 sequence contains 29903bp, which includes 14 open reading frames (ORFs) coding for the replicase ORF1ab, Spike (S), Envelope (E), Membrane (M) and Nucleocapsid (N) structural proteins, and several non-structural (nsps) and accessory proteins (9, 10). The Spike on the surface of the virus is responsible for the attachment and invasion of host cells (11). Spike is a highly glycosylated trimeric class I fusion protein and contains two subunits, S1 and S2 (12). CryoEM studies showed that it remains in a metastable pre-fusion conformation with a hinge-like movement of the S1 subunit, which attaches by the Spike receptor binding domain to host cells that express the angiotensin-converting-enzyme 2 (ACE2) receptor. After attachment, the S1 sheds and leaves the S2 subunit in a stable post-fusion conformation. The latter mediates membrane fusion and is responsible for the invasion of the host cell (13, 14).

The ACE2 appears to be the molecular entryway to the host (13, 15-17), as the SARS-CoV-2 Spike binds to this receptor. The virus requires priming proteolysis by the TMPRRS2 serine protease, which attacks a furin-like cleavage site on the S protein. The conformational change then stabilizes the complex, allowing the virus to infect the host cell (18, 19). The presence of ACE2 has been confirmed in different tissues (20-22), that are related to clinical manifestations of COVID-19 (23). This mechanism mediated by S glycoprotein highlights the importance of this protein as a target for the development of therapies such as neutralizing antibodies and vaccines (24-28). In this sense, isolation of specific antibodies could be instrumental in the development of effective diagnostic and therapeutic tools against the virus.

Some naturally occurring antibodies that lack light chains are known as single-domain antibodies (HCAb). They are derivates of IgG and occur in the entire camelidae family (29). The camelidae family comprises of camels, dromedaries, llamas, vicuñas, guanaco, and alpacas (30). The antigen-binding fragment of an HCAb contains a single variable VHH domain consisting of 3

hypervariable regions. When isolated, the VHH domain is also known as a Nanobody. Nanobodies can be used as therapeutic bullets against tumors, pathogens, and chronic diseases (31-33). Nanobodies are in general more stable than conventional antibodies and their expression is efficient in the periplasm. In fact, several milligrams can be produced from one liter of culture (31, 34-37). More novel strategies using Nanobodies as intrabodies to target specific proteins for selective degradation might allow the therapeutic ablation of intracellular targets (38-40).

Nanobodies derived from camelid HCAbs are obtained after immunization with the target protein plus adjuvant. Our platform has developed an improved procedure for the production of Nanobodies using Alpacas as donor species. To isolate the genetic sequences of the target-specific Nanobodies produced after immunization, peripheral blood B-lymphocytes are isolated to obtain total RNA, followed by cDNA preparation to finally amplify the Nanobody region (41). The cDNA fragment encoding the Nanobody is as short as 360nt, and up to ~ $3x10^6$ single clones can be obtained from 120 mL blood: a safe and harmless procedure for our alpacas. Afterward, a bacterial display system was used to clone the full single Nanobodies. Here, we report an optimized, fast, efficient, inexpensive and simple density gradient method for Nanobody selection, and a sub-nanomolar affinity Nanobody against the Spike receptor binding domain of SARS-CoV-2.

Results

The process of classic nanobody generation and selection takes months. For instance, full immunization requires on average 8 weeks, and the process also comprises the construction of the Nanobody library and affinity selection of clones, which can take an additional 6 months. Here we show a method to fast track immunization of an alpaca with the full-length Spike of SARS-CoV-2. We obtained the lyophilized protein raised in a baculovirus expression system. Previous to immunization, protein integrity was tested by SDS-Page and Coomassie staining (Figure 1a). Then, an alpaca called Buddha (Figure 1b) was immunized twice over 14 days with 100 µg of the

full Spike protein. The animal´s health was monitored throughout the study period by clinical examination, hematology analysis, and serum biochemistry. The immune response of the alpaca´s serum before immunization revealed a fortunate basal cross-reaction against the Spike protein, and after the second immunization, we observed a significant increase of IgG antibodies in the alpaca´s serum. This was done in a rapid qualitative manner by Dot blot analysis, immobilizing the epitope to a nitrocellulose membrane and using alpaca serum as a source of primary antibodies (Figure 1c). We also detected IgG antibodies by ELISA using the full Spike protein immobilized to the plate with the alpaca´s serum as a source of primary antibodies (Figure 1d). The Bacterial Display system takes advantage of the high-efficiency of transformation of *E. coli* and avoids the need of bacteriophage infections or shuttling into yeast cells for surface display of the Nanobodies (42). Importantly, this Nanobody display system can drive the specific adhesion of *E. coli* bacteria to abiotic and cellular surfaces with the cognate antigen (43, 44). Thus, we rapidly constructed a bacterial display library with a complexity of 2.3 $x10^6$ independent clones was quickly achieved by a electroporation of *E. coli* DH10B-T1R strain with 0.7% religation of the vector(44-46) (see Materials and Methods).

We applied a novel procedure for the selection of Nanobodies based on a simple Ficoll density gradient, an inexpensive reagent available all around the world used for blood fragmentation. We were inspired by the main observation that red cells accumulate at the bottom of the Ficoll density gradient, while PBMCs stay in the upper fraction. Using conventional NHS-activated Sepharose beads in a Ficoll gradient, we found that the density of the beads was sufficient to precipitate to the bottom of a 15mL tube. Further, the same assay was performed with free bacteria, and as expected the bacteria remained in the upper fraction. Since a single Nanobodies type is expressed by every bacterium of the library(42). In the bacteria display system used, *E. coli* bacteria express upon IPTG-induction intimin-Nanobody protein fusions that anchor in the outer membrane and expose the functional Nanobody to the extracellular milieu for antigen recognition. These intimin-Nanobodies fusions also contain a common epitope (myc-tag) at the C-terminus for

immunodetection (45). Therefore, we hypothesized that bacteria expressing specific Nbs on their surface would bind NHS-beads coated with the protein of interest (i.e. Spike SARS-CoV-2) and will migrate all the way through to the bottom of the Ficoll density gradient, leaving unbound bacteria in the upper fraction (Figure 1e). Indeed, we demonstrated that specific Nanobodies from a bacterial display library can be rapidly and inexpensively selected with our protocol using common reagents and a conventional centrifuge. A full description is provided in the Methods section.

We optimized conditions to extract the intimin-Nanobody fusions from the bacterial outer membrane and used these protein extracts directly for assaying binding to Spike protein applying two different methods: Dot blot analysis and high-content microscopy: For Dot blot analysis and High-content microscopy. After nanobody selection using our simple Ficoll based density gradient protocol, we obtained ~ 1000 colonies on LB-agar plates from the Sepharose-antigen coated fraction. 100 colonies were analyzed, the bacteria were inoculated in liquid LB media and further induce the expression of intimin-Nanobody of single clones. Bacterial pellets were lysed under optimized conditions and the extract was used as a source of Nanobodies -as primary antibodies- for the second binding screening. For Dot blot analysis a negative control of an unrelated protein was applied next to the same amount of full-length Spike on the nitrocellulose strips. Single Dot blot strip tests were incubated with the bacterial extracts containing Nanobodies. Nanobodies binding to Spike were unveiled by sequential incubation with mouse anti-myc antibody and an anti-mouse HRP-conjugate. Of the first 100 clones, we focus on two strongly bound to the full-length Spike in the Dot blot analysis (W23UACh and W25UACh). Furthermore, we used high content microscopy as a second confirmation method. Therefore, a single 10 cm-plate was transfected with a Spike-GFP vector for 24h, and cells were seeded onto 96 well-plates. After 24 hours, the cells were fixed, permeabilized, and individual extracts of our 100 selected bacterial display clones were incubated as a source of Nanobodies. Nanobodies were myc tagged after incubation with a mouse anti-myc antibody and an anti-mouse Alexa647 secondary antibody was

used for immunofluorescence assays. HeLa cells had a transfection efficiency of ~20%. In this case, a low transfection rate is desired because it allows us to evaluate unspecific binding to un-transfected cells in the same image. Consistent with the Dot blot analysis, the W23UACh and W25UACh Nanobodies bound to the Spike-GFP expressed in human cells (Figure 2b). We observed colocalization of W23UACh and W25UACh to Spike-GFP, while no colocalization was observed with negative control extracts (Figure 2b). We also observed that W25UACH does not bind to the nucleoprotein of SARS-CoV-2 tagged to a GFP protein (Supplemental Figure-1b): confirming that W25UACh binds specifically to Spike and not to GFP. The selected clones were sequenced and the alignment of the amino acid sequences showed a high similarity between the two nanobodies, CDR3 was exactly the same in both antibodies, therefore we concluded the two nanobodies are members of the same family and were most likely generated from a common origin during the Alpaca´s immunoreaction against the Spike protein (Figure 2c). Here we have presented a method that rapidly performs secondary screening selection of Nanobodies, using bacterial extracts from selected clones of the bacterial display library, using either conventional biochemical methods such as Dot blot analysis or high content microscopy immunofluorescence-based assays.

After cloning the W25UACh nanobody into the pHen6 vector for periplasmic bacterial expression large amounts of purified W25UACh nanobody were obtained (Supplemental Figure-1c & 1d). We demonstrated a direct interaction between the Spike RBD and the W25UACh nanobody by pulldown assay, with pure recombinant RBD protein or BSA protein as a control. The above were covalently immobilized to NHS-Sepharose beads, further binding to W25UACh was tested to RBD and control beads, and we showed that the selected W25UACh nanobody binds to RBD (Figure 3a). The purified W25UACh nanobody was used for immunofluorescence of HeLa cells transiently transfected with a Spike tagged to a GFP vector in Figure 3b. The W25UACh nanobody specifically recognized the Spike-GFP in a sensitive manner (Figure 3b), given that we observed colocalization of Spike-GFP and W25UACh to ruffles in HeLa cells (Figure 3b). Thus, our

experiment suggests the use of the W25UACh nanobody as a measure for the direct diagnosis of infected cells by immunofluorescence. We demonstrated proper folding of the RBD domain and the nanobody using a label-free Tycho measurement, yielding inflection temperatures (T_i) of 52.4°C and 57.9°C which is indicative of thermal stability. Mixing the RBD domain with the nanobody led to strong thermal stabilization of the RBD domain at around 14°C, thus confirming the tight interaction between the RBD domain and the nanobody (Figure 3c). To finally quantify the interaction affinity between the RBD domain and W25UACh, Microscale Thermophoresis (MST) was applied. The MST experiment resulted in an affinity of W25UACh for the RBD domain of 295 ± 84 pM (Figure 3d). Thus, our procedure using simple gradient selection can select sub-nanomolar affinity Nanobodies against the RBD domain of the Spike of SARS-CoV-2.

Discussion

Currently selection of nanobodies from bacterial display is performed by affinity purification based on magnetic beads binding the labelled antigen or by FACS Sorter or selection on cells transfected with the antigen (46). Herein, we describe a novel simple method for the selection of Nanobodies from *E. coli* bacterial display libraries. Our method used only conventional laboratory instruments and an inexpensive Ficoll gradient for the selection of Nanobodies from a highly complex and diverse bacterial library. The success rate depends on the immune response of the alpaca to the epitope. Nevertheless, which in this case could have been unwittingly aided by prior undetermined exposure to cross-reactive camelid coronaviruses (47-49). Nevertheless, here we have shown a successful example based on an immunization program of two week´s duration and 100 clones analysis; thus, our methods can accelerate the identification of nanobodies, enabling the generation of diagnostic and potentially therapeutic measures against Covid-19 and other infectious and emergent viruses.

The medical, social, and economic consequences of COVID-19 impact the lives of everyone on the planet and while vaccines and effective therapies are not available, sensitive diagnostic tools are urgently needed. Currently, convalescent plasma transfusion has been applied as an emergency treatment for COVID-19, aiming to enhance the immune response of the patients (50, 51). In the late phase of disease progression, an inflammatory cytokine storm has been reported. Antibody administration at this stage by convalescent plasma transfusion is under discussion, especially for critically ill patients (52). Nanobodies might become an alternative for immunotherapy to replace or complement convalescent plasma transfusion. Here we characterized the affinity properties of novel Nanobodies against the Spike protein of SARS-CoV-2. We demonstrated that W25UACh could be suitable for diagnostic and pathology studies since it can detect Spike expressed in human cells, the yield of production of W25UACh is high and inexpensive; several milligrams of the Nanobody can be obtained from a single liter of bacterial culture as shown in the Supplemental Figure 1C. Using fast thermal denaturation, we were able to determine the folding of RBD and W25UACh with a T_i of 52.4°C and 57.9°C, respectively. Clear evidence of binding between these two proteins is the Ti shift to 66.8°C, stabilizing at ~14°C: further determined by Thermophoresis that the Nanobody W25UACh affinity for the RBD domain of Spike is K_D ~295 ± 84 pM. The other three research groups have been reported Nanobodies against Spike RBD: VHH 72 with an K_d of 39nM (53), Ty1 with an K_d of 8 ± 1.5 nM at normal salt conditions (54), and a large set over eighteen humanized single-domain antibodies, across the selected antibodies the highest affinity was shown by the clone n3021 K_d of 0.63 ±0.01 nM. Thus, to date the monomeric W25UACh Nanobody reported here shows the highest affinity for the Spike protein of SARS-CoV-2, however further experiments are needed to determine whether W25UACh can also neutralize the infection of cells by disrupting the interaction of Spike RBD to the ACE2 cellular receptor.

In a nutshell, we provide a powerful method to accelerate the generation of Nanobodies against pathogens and a sub-nanomolar affinity nanobody obtained against the Spike protein of SARS-CoV-2.

Material and Methods

Immunization and VHH library construction

The alpaca immunization process followed the protocol the guidelines established by the Bioethics Committee of the Austral University of Chile certifications 338/2019 and 388/2020. One day before immunization, 5 mL of blood was collected for pre-immune serum tests. For immunization (day 1), 100 µg of full-length Spike protein of SARS-CoV-2 (SINOBiological) was used. The cold lyophilized protein was dissolved in 2 mL of adjuvant (Veterinary Vaccine Adjuvant, GERBU FAMA) diluted 1:1 in sterile water and injected subcutaneously into a male alpaca (*Vicugna pacos*). A total volume of 4 mL was injected into four different locations in the alpaca. A 5 mL blood sample was collected seven days after the first immunization. On day 14, the alpaca was immunized again with 100 µg Spike, and on day 15 a sample of 120 mL blood was collected from the jugular vein in tubes containing 3.8% sodium citrate as an anti-coagulant. The uncoagulated blood sample was mixed with the same volume of HBSS medium without calcium (Gibco), divided into aliquots of 10 mL and each aliquot was added on top of a 5 mL of Ficoll-Paque Premium (GE Healthcare) in 15 mL sterile Falcon tubes. After centrifugation (1.200 × rpm, 80 min, RT), the PBMC fraction was recovered from the interphase, washed twice in PBS by centrifugation (3.500 × rpm, 10 min), resuspended in 4 mL of sterile PBS (Gibco). RNA extraction and cDNA production were performed using the commercial RNeasy Mini Kit (Qiagen) and QuantiTect Reverse Transcription Kit (Qiagen) respectively according to the manufacturer's instructions. Approximately 2 µL of each cDNA synthesis procedure were used as templates in 50 µL PCR reactions with oligonucleotides CALL001 (5´-GTC CTG GCT CTC TTC TAC AAG G-3´) and CALL002 (5´-GGTACGTGCTGTTGAACTGTTCC- 3´)(55). The amplified fragments of ~0.6 kb,

corresponding to VHH-CH2 domains, and ~0.9 kb, corresponding to conventional VH-CH1-CH2 domains, were separated in 1.2% (w/v) low melting agarose gels and the ~0.6 kb band was purified (QIAEX II Gel Extraction kit, Qiagen). This fragment was used as a template in a second PCR reaction with oligonucleotides VHH-Sfi2 (5´-GTC CTC GCA ACT GCG GCC CAG CCGGCC ATG GCT CAG GTG CAG CTG GTG GA-3') and VHH-Not2 (5´- GGA CTA GTG CGG CCG CTG AGG AGA CGG TGA CCT GGG T-3´) to finally obtain the amplified fragments of ~0.4 kb, corresponding to VHH domains. The amplified VHH fragments were digested with SfiI and NotI (Thermo Scientific) restriction enzymes and ligated into the same sites of the purified vector pNeae2 (46). Ligations were electroporated in E. coli DH10B-T1 R cells obtaining a library size of ~3×10^6 individual clones, as determined by plating on LB-Chloramphenicol agar plates with 2% w/v glucose incubated at 30°C. Less than 0.7% of re-ligated vectors were estimated from a control ligation performed in parallel without the DNA insert. Transformed bacteria were scraped from plates and stored at -80°C in LB broth with 30% glycerol.

Coupling epitopes to beads

1 mL of NHS-activated sepharose 4 Fast Flow beads were washed with 2 mL of cold 1 mM HCl immediately before use, then washed 5 times with cold sterile PBS. 200 µg of purified protein in PBS 1X was added to the beads and incubated with rotation overnight. Non-reacted groups in the medium were blocked by adding ethanolamine to a final concentration of 0.5 M. Beads were washed 5 times with PBS and stored at 4°C.

ELISA Assay

10 ng of SARS-CoV-2 Spike protein diluted in PBS 1X pH 7,4 were bound in each well of the ELISA Plate, incubated at 37°C for 1h. Followed by a 3 x 5 min wash with PBS-T(PBS 0.1% Tween20). Serial dilutions (1:5000in PBS 1X) of Pre and Post immunization serum were incubated at 37°C for 1h. Followed by a 3 x 5 minutes wash with PBS-T. Secondary detection

was done with peroxidase-labeled anti- Llama IgG (1:5000 in PBS-T), followed by a 3 x 5 min wash with PBS-T and visualized using 1-step Ultra TMB-ELISA (THERMO), 5 min at 37°C. Signal was measured at 650nm in a microplate reader after 10 min incubation.

Density gradient separation

1 mL of glycerol stock from the library was inoculated in a flask containing 20 mL of LB medium with 25 µg/mL of chloramphenicol and 2% glucose. The flask was incubated (pre-inoculum) overnight at 37ºC with 200 rpm agitation. The same procedure was repeated with control bacteria that were transformed with a kanamycin resistant plasmid (negative control). The pre-inoculum was pelleted and resuspended in LB medium with 25 µg/mL chloramphenicol and then diluted to 0.02 OD600 in 100 mL of fresh LB medium with 25 µg/mL chloramphenicol without glucose, incubated at 37ºC with 200 rpm agitation until it reached 0.45 - 0.6 OD600. IPTG was added to a final concentration of 50 µM to induce protein expression for 3 hours at 30ºC and 200 rpm. OD600 absorbance of library and control bacteria cultures was measured. 50 mL of both cultures was washed three times with 10 mL of filtered PBS. Centrifugation was always performed at 3000 x g for 5 min. Libraries culture (chloramphenicol resistant) and the negative control (kanamycin resistant) were resuspended in a final volume of 10 mL PBSX. 2 mL of library culture and 2 mL of negative control cultures were mixed (if final OD600nm were same, if not the volume of the control bacteria was adjusted based on OD in order to add an equal amount of bacteria) and incubated with 300 µL of NHS beads coupled to epitope protein on a 15 mL conical tube on a rocking platform for 30 min at room temperature. The mixture was slowly added on the top of 6 mL of Ficoll (Ficoll-PaqueTM PLUS GE Healthcare) in a 15 mL conical tube, centrifuged at 200 x g for 1 min. The unbound fraction was discarded (upper fractions), leaving a visible pellet of beads that was resuspended in 4 mL PBS and rotated for 5 min at room temperature. This step was repeated six times. Finally, 1 mL of LB medium was added and incubated for 5 min at room temperature, then 50 µL were plated on LB agar plates with 50 µg/mL kanamycin and 2% glucose, 50 µL were plated

on LB agar plates with 25 µg/mL chloramphenicol and 2% glucose and the rest in at least two LB chloramphenicol/glucose agar plates, incubated at 37ºC overnight (>20hrs recommended). The colony number of the first two plates were counted as a measurement of specific enrichment of Nanobodies expressing bacteria from the library.

Expression, sub-cloning and purification of Nanobodies

The selected VHH cDNA fragments were digested with SfiI and NotI (Thermo Scientific) restriction enzymes and ligated into the same sites of the purified vector pHen6 (56). For periplasmic expression the E. coli wk6 strain was used, the pHen6-W25UACh vector was transformed and a single clone was selected from the agar plates and inoculated in 20 mL of liquid LB-medium containing 100µg/ml ampicillin and glucose 1%. The bacteria were cultured at 37 °C with agitation for 16 h. The cells were then diluted into 1L Terrific Broth (TB) medium containing 100µg/ml ampicillin, 2mM MgCl2, 0,1% glucose and grew at 37 °C to an OD600 of 0.6–0.9. The expression of the nanobodies was induced by adding 1 mM of IPTG (isopropyl-β-d-1-thiogalactopyranoside) for 20h at 28 °C. Cells were collected by centrifugation at 8000 rpm for 8 min at 4 °C. The harvested cells were resuspended in a 12 mL TES buffer (0.2 M Tris pH 8.0, 0.5 mM EDTA, 0.5 M sucrose) and incubated for 1h on ice, then incubated for another hour on ice in a 18 mL TES buffer, diluted 4 times and centrifuged at 8000 rpm at 4°C to pellet down cell debris. The supernatant was loaded on 5mL of HisPur Ni-NTA agarose resin which was pre-equilibrated with binding buffer (Tris 50mM, NaCl 500 mM, imidazole 10 mM pH 7,5). The lysed cells containing His tagged nanobodies were added to the column followed by adding the column´s volume in binding buffer for a total of 8 times. The column was washed by adding 8-fold the column´s volume with wash buffer (Tris 50mM, NaCl 500 mM, imidazole 30 mM pH a 7.5), and eluted with 15mL of elution buffer (Tris 50mM, NaCl 150 mM, 150 mM imidazole, 1mM DTT pH 7.5). Purified nanobodies were verified by SDS-PAGE Coomassie staining analysis.

In vitro Pulldown assay

100 µL of recombinant W25UACh (1 µg/µL) was incubated with 100 µL NHS-activated sepharose 4 Fast Flow beads coupled to SARS-CoV-2 Spike protein plus 800 µL of PBS1x pH 7,4 and bovine serum albumin coupled beads (negative control) for 1 h at room temperature, followed by 3 x 3 h wash with PBS-T(PBS 0.1% Tween20), 3 x 5 min wash with PBS 500 mM NaCl and 3 x 5 min wash with PBS 1X . The pulled down materials were boiled in Laemmli sample buffer, separated by 10% SDS-polyacrylamide gels and stained with coomassie blue. Recombinant SARS-CoV-2 (2019-nCoV) Spike S1 Protein (RBD) from Trenzyme, Germany was used for the assays.

Cell culture

HeLa were maintained at 37°C in DMEM/F12 supplemented with 10% FCS and 100 units/mL of penicillin and streptomycin. Plasmid transfection was performed in 10 cm plates using 25 µg of DNA, 24h after transfection cells were split into 96 well plate ~10000 cells per well. Transfection was performed using Lipofectamine 2000 (Invitrogen) according to the manufacturer's instructions and media were supplemented with Normocin during transfection (Invivogen).

Dot Blot analysis screening

Individual colonies obtained from a density gradient separation protocol were inoculated into 2 mL of LB medium and incubated overnight at 37ºC with 200 rpm agitation. 100 µL of Pre-inoculum was added to 1.9 mL of fresh LB medium with 25 µg/mL chloramphenicol, incubated at 37ºC with 200 rpm agitation until it reached 0.45-0.6 OD600. To induce protein expression IPTG was added at a final concentration of 50 µM for 3 h at 30ºC and 200 rpm. The culture was pelleted and resuspended in 1mL PBS 1X 0.2% TritonX100, sonicated for 10 seconds at 40% on ice, then centrifuged at 14.000 x g for 30 mins at 4°C and the supernatant was recovered to obtain a total

protein extract from each clone. 1 µl of protein SARS-CoV2 Spike protein (200 ng/uL) and a E. coli total protein extract were spotted within a pre marked grid onto a 0.2 µm pore–size nitrocellulose membrane (Merk Millipore). The membrane was left to dry to fix the proteins for 30 min at room temperature. Non-specific sites were blocked with blocking solution (PBS- 0.1% Tween20 with 5 % bovine serum albumin) for 30 min at room temperature with agitation. The blocking solution was discarded and each membrane was incubated for 1 h at room temperature with agitation at a dilution of 1:10 for the total protein extract of each clone in 5 ml of TBS-T containing 5% BSA, followed by 3 x 5 min wash with PBS-T. Secondary antibody incubation was performed with Mouse Anti-Myc antibody (9B11, Cell Signalling) 1:3000 in PBS-T containing 5% BSA for 1 h at room temperature, followed by 3 x 5 min wash with PBS-T. After this, the membrane was incubated with a Goat anti mouse IgG antibody coupled to HRP (Invitrogen) 1:5000 in PBS-T containing 5% BSA, for 1h at room temperature, followed by 3 x 5 min wash with PBS-T and visualized using the ECL reagent (Pierce).

High content microscopy

Cells were grown on a 96 well optical plate (Themofisher) were washed with PBS 1X 3 times and fixed with 4% paraformaldehyde at room temperature for 30 min. After fixation, cells were washed with PBS 1X and permeabilized in PBS 0.2% Triton X 100. After washing the cells 3 times in PBS 1X they were then incubated to either extract containing Nanobodies or Purified Nanobodies during 45 minutes at 37°C, after further washing another 3 times with PBS 1Xa secondary anti-myc (Cell Signaling) was used at 1:3000 and incubated during 45 minutes at 37°C. Directly afterward the cells were washed 3 x times in PBS 1X and incubated with an anti-mouse Alexa 647 during 35 minutes at 37 C. For nuclei staining, cells were washed with PBS 1X and incubated for 10 min at room temperature with 0.1 mg/mL DAPI. After the final wash, cells were maintained in the 96 well optical plates in 100 uL PBS 1X. Images of fixed cells were acquired with a high content automatic microscope, Celldiscoverer 7 (Carl Zeiss GmbH, Jena, Germany).

Structural integrity and functionality tests using Tycho NT.6.

The binding of W25UACh and the structural integrity of Spike RBD was verified using a label-free thermal shift assay with Tycho NT.6 (Nanotemper Technologies GmbH) using intrinsic Tryptophan and Tyrosine fluorescence. 10 µL solutions of Spike RBD (2 µM), W25UACh (2 µM) and Spike RBD mixed with W25UACh (2 µM each) were prepared and loaded into Capillaries Tycho NT.6 (TY-C001, NanoTemper Technologies GmbH). The Tycho instrument applies a quick thermal ramp from 35°C to 95°C with a heating rate of 30°C/min and the unfolding of proteins can be monitored through changes in the 350 nm / 330 nm fluorescence emission ratio. Recombinant SARS-CoV-2 (2019-nCoV) Spike S1 Protein (RBD) from Trenzyme, Germany was used for the assays.

Binding affinity measurements using MST.

For the dissociation constant (Kd) between the W25UACh nanobody and SARS-CoV-2 S1, Spike RBD was measured by microscale thermophoresis (MST) using a Monolith NT.115PICO instrument (Nanotemper Technologies GmbH). Purified W25UACh was buffer exchanged into a PBS buffer, pH 7.4, and its concentration was adjusted to 10 µM using UV-absorbance. Next, W25UACh was fluorescently labeled with the Monolith Protein Labeling Kit RED – NHS 2nd Generation (MO-L011, NanoTemper Technologies GmbH) following the protocol established in the manual. Labeled W25UACh was centrifuged at 14,000 rpm for 15 min to eliminate precipitates. A 16-point serial dilution series of recombinant Spike RBD (250 nM – 7.6 pM) was applied in PBS buffer containing 0.01% Pluronic F-127 and mixed with a final concentration of 1 nM labeled W25UACh. Affinity measurements were conducted in Premium Capillaries Monolith NT.115 (MO-K025, NanoTemper Technologies GmbH) and repeated three times. Recombinant SARS-CoV-2 (2019-nCoV) Spike S1 Protein (RBD) from Trenzyme, Germany was used for the assays.

Author Contributions Statement

Immunization and animal wellbeing T.P, B.U and C.D; Bacterial display and gradient protocol development G.V.N, R.J, J.H, C.S, T.P, N.L.G.R, Z.M.C, Y.C, A.C, L.A.F, Y.M, S.G.M, H.M, A.M, B.U, P.K, P.E, J.B, P.C.C, L.A.F & A.R.F; SARS-CoV-2 PBMCs isolation T.P & J.H; libraries construction J.H & R.J, Nanobodies selection Y.M, L.A.F, R.J & G.V.N, Nanobodies binding confirmation G.V, J.H & A.R.F, Nanobodies expression Y.C & R,J; Conceptualization, A.R.F, G.V, R.J, L.A.F & C.S, Data curation, G.V.N, R.J, J.H, C.S, T.P, N.L.G.R, Z.M.C, Y.C, A.C, A.R.F; Formal analysis A.R.F, G.V & R.J, Funding acquisition P.K, J.B, A.M, B.U, P.C.C, G.R & A.R.F; Resources J.B, A.M, B.U, P.C.C, G.R & A.R.F, Supervision A.R.F; Writing—original draft, L.A.F, A.R.F, G.V & R.J; Writing—review and editing, G.V.N, R.J, J.H, C.S, T.P, N.L.G.R, Z.M.C, Y.C, A.C, L.A.F, Y.M, S.G.M, A.M, B.U, P.K, P.E, G.R & A.R.F. All authors have read and agreed to the published version of the manuscript.

Acknowledgment

The authors would like to thank the KOICID for partially supporting this study. We thank Dr. Ronald T. Hay for his generous support and assistance. This work was funded by FONDECYT No. 11150532 to ARF; FONDEF No ID17I10037 to ARF; FONIS EU-LAC T010047 to PCC, JO, JB, NLR & ARF; PAI-CONICYT No 79150075 to ARF; FONDEQUIO EQM180037 to ARF; the regional Council of the “Los Rios region” project FICR16-19 and FICR19-20; J.B was funded by ISCIII Miguel Servet Program CP19/00200. Graduate fellowship ANID Nº 21161365 to R.J; ANID Nº21160481 to A.C; ANID Nº 22170632 to C.S; Z.M.C was funded by the academic graduate students fellowship of the University of Costa Rica of the academic mobility program; N.L.G.R was funded by Becas Santander Iberoamerica Investigacion 2018/2019; H.M was funded by a postdoctoral fellowship from FONDECYT 3170159. Work in the laboratory of L.A.F is supported

by Grants BIO2017-89081-R (Agencia Española de Investigación AEI/MICIU/FEDER, EU) and CSIC PIE-RDL-COVID-19 (Ministerio de Ciencia e Innovación from Spain). We thank Dzongsar Khyentse Rinponche for his generous donation of alpacas to this project. We would like to thank Amber Philp for proofreading and Rocio Miranda, Andrea Bastidas, Vanessa Wiederhold, and Viviana Estrada for administrative support, and Omer Navarrete for his commitment to the wellbeing of the Alpacas.

Conflict of interest statement

The Austral University of Chile claiming priority to U.S. Provisional Patent Application No. US Serial No. 63/025534, filed MAY-2020.

Resource Availability

Requests for reagents may be directed to Alejandro.Rojas@uach.cl. All reagents generated in this study are available according a Materials Transfer Agreement.

Figure Legends

Figure-1. Immunization of the Spike of SARS-CoV-2 and a simple density gradient method for the selection of Nanobodies

A) SDS- Page to ensure protein integrity of full-length Spike of SARS-CoV-2 before immunization. **B)** Adult alpaca immunized with Spike**. C)** Evaluation of the alpaca´s immune response by Dot blot. Image shows the reaction to decreasing amounts of Spike-1 and Bovine serum albumin (negative control) using a pre-immunization control, and after one immunization (1 week), or two immunizations (3 weeks) with full-length SARS-CoV-2 Spike, using alpaca serums as a primary antibody source followed by an anti-camelid IgG-HRP secondary antibody. **D)** ELISA assay before and after the second immunization (3 weeks). **E)** Schematic representation of novel protocol for isolation of Nanobodies using density gradient separation. The bacterial display library expressing the Nanobodies on the surface of bacteria is briefly incubated with conventional Sepharose beads coated with the epitope of interest. Directly after the mixture is deposited on a Ficoll gradient conic tube and centrifuged at 200 x g for 1 min, the beads drive through the gradient to the bottom of the tube with the bacteria expressing specific Nanobodies, while the unbound bacteria remain on the surface of the gradient. The beads are then resuspended, and bacterial clones are isolated for biochemical binding confirmation.

Figure-2. Dual biochemical and microscopy-based selection fo Nanobodies A) Dot blot immunodetection of full-length SARS-CoV-2 Spike using direct total protein extracts of clones W25UACh and W23UACh as the primary antibody. Mouse anti-Myc 1:3000 followed by anti-Mouse-HRP were used for detection. Protein extract from E. coli (BL21 strain) was used as a negative control. **B)** Immunodetection of Spike-GFP transiently transfected in HeLa cells using

total protein extract selected clones as the primary antibody, followed by Mouse anti-Myc 1:3000 and anti-Mouse-Alexa 647. The image shows two positive clones W25UACh and W23UACh, and an example of a negative nanobody. **C)** Sequence alignment of W25UACh and W23UACh predicted aminoacidic sequence. CDR sequences are marked with a black line.

Figure-3 Binding Characterization of W25UACh to SARS-CoV-2 Spike. A) Pulldown of the W25UACh nanobody, a recombinant Spike RBD domain of the SARS-CoV-2 Spike protein or control BSA protein was covalently bound to NHS- Sepharose beads. Further, the W25UACh nanobody was incubated with control and Spike RBD beads, washed, and further eluted in LSD lysis buffer (Invitrogen). **B)** HeLa cells were transiently transfected with full-length Spike-GFP and immunofluorescence was performed with the pure W25UACh nanobody, showing increased resolution of Spike visualized on a Celldiscoverer7 microscope. **C)** Unfolding profiles of 2 μM SARS-CoV-2 S1, Spike RBD in the absence (black) and presence (red) of 2 μM W25UACh, measured with Tycho NT.6. Binding of W25UACh to Spike RBD leads to strong stabilization and shifts the inflection unfolding temperature (T_i) from 52.1°C to 66.3°C. **D)** MST binding curve for the titration of 1 nM fluorescently labeled W25UACh into a 16-point serial dilution of SARS-CoV-2 S1, Spike RBD (250 nM – 7.6 pM). W25UACh binds Spike RBD with sub-nanomolar affinity (K_d = 295 ± 84 pM). Error bars show the SD calculated from experiments performed in triplicate.

References

1. Gorbalenya AE, Baker SC, Baric RS, de Groot RJ, Drosten C, Gulyaeva AA, et al. The species Severe acute respiratory syndrome-related coronavirus: classifying 2019-nCoV and naming it SARS-CoV-2. Nature Microbiology. 2020;5(4):536-44.
2. Awadasseid A, Wu Y, Tanaka Y, Zhang W. Initial success in the identification and management of the coronavirus disease 2019 (COVID-19) indicates human-to-human transmission in Wuhan, China. Int J Biol Sci. 2020;16(11):1846-60.
3. Kong WH, Li Y, Peng MW, Kong DG, Yang XB, Wang L, et al. SARS-CoV-2 detection in patients with influenza-like illness. Nat Microbiol. 2020;5(5):675-8.
4. WHO. Coronavirus Disease (COVID-19) Situation Report-103. World Health Organization, Department C; 2020. Report No.: 103.
5. Hartley DM, Perencevich EN. Public Health Interventions for COVID-19: Emerging Evidence and Implications for an Evolving Public Health Crisis. JAMA. 2020.
6. Zhang J, Litvinova M, Liang Y, Wang Y, Wang W, Zhao S, et al. Changes in contact patterns shape the dynamics of the COVID-19 outbreak in China. Science. 2020:eabb8001.
7. Marra MA, Jones SJ, Astell CR, Holt RA, Brooks-Wilson A, Butterfield YS, et al. The Genome sequence of the SARS-associated coronavirus. Science. 2003;300(5624):1399-404.
8. Zhou P, Yang X-L, Wang X-G, Hu B, Zhang L, Zhang W, et al. A pneumonia outbreak associated with a new coronavirus of probable bat origin. Nature. 2020;579(7798):270-3.
9. Wu F, Zhao S, Yu B, Chen Y-M, Wang W, Song Z-G, et al. A new coronavirus associated with human respiratory disease in China. Nature. 2020;579(7798):265-9.
10. Wu A, Peng Y, Huang B, Ding X, Wang X, Niu P, et al. Genome Composition and Divergence of the Novel Coronavirus (2019-nCoV) Originating in China. Cell Host & Microbe. 2020;27(3):325-8.
11. Lan J, Ge J, Yu J, Shan S, Zhou H, Fan S, et al. Structure of the SARS-CoV-2 spike receptor-binding domain bound to the ACE2 receptor. Nature. 2020;581(7807):215-20.
12. Wrapp D, Wang N, Corbett KS, Goldsmith JA, Hsieh CL, Abiona O, et al. Cryo-EM structure of the 2019-nCoV spike in the prefusion conformation. Science. 2020;367(6483):1260-3.
13. Wrapp D, Wang N, Corbett KS, Goldsmith JA, Hsieh C-L, Abiona O, et al. Cryo-EM structure of the 2019-nCoV spike in the prefusion conformation. Science. 2020;367(6483):1260-3.
14. Walls AC, Park Y-J, Tortorici MA, Wall A, McGuire AT, Veesler D. Structure, function and antigenicity of the SARS-CoV-2 spike glycoprotein. bioRxiv. 2020:2020.02.19.956581.
15. Luan J, Lu Y, Jin X, Zhang L. Spike protein recognition of mammalian ACE2 predicts the host range and an optimized ACE2 for SARS-CoV-2 infection. Biochemical and Biophysical Research Communications. 2020;526(1):165-9.
16. Lan J, Ge J, Yu J, Shan S, Zhou H, Fan S, et al. Structure of the SARS-CoV-2 spike receptor-binding domain bound to the ACE2 receptor. Nature. 2020.
17. Shang J, Ye G, Shi K, Wan Y, Luo C, Aihara H, et al. Structural basis of receptor recognition by SARS-CoV-2. Nature. 2020.
18. Hoffmann M, Kleine-Weber H, Schroeder S, Krüger N, Herrler T, Erichsen S, et al. SARS-CoV-2 Cell Entry Depends on ACE2 and TMPRSS2 and Is Blocked by a Clinically Proven Protease Inhibitor. Cell. 2020.

19. Coutard B, Valle C, de Lamballerie X, Canard B, Seidah NG, Decroly E. The spike glycoprotein of the new coronavirus 2019-nCoV contains a furin-like cleavage site absent in CoV of the same clade. Antiviral Research. 2020;176:104742.
20. Li G, He X, Zhang L, Ran Q, Wang J, Xiong A, et al. Assessing ACE2 expression patterns in lung tissues in the pathogenesis of COVID-19. Journal of Autoimmunity. 2020:102463.
21. Xu H, Zhong L, Deng J, Peng J, Dan H, Zeng X, et al. High expression of ACE2 receptor of 2019-nCoV on the epithelial cells of oral mucosa. International Journal of Oral Science. 2020;12(1):8.
22. Hikmet F, Méar L, Uhlén M, Lindskog C. The protein expression profile of ACE2 in human tissues. bioRxiv. 2020:2020.03.31.016048.
23. Lamers MM, Beumer J, van der Vaart J, Knoops K, Puschhof J, Breugem TI, et al. SARS-CoV-2 productively infects human gut enterocytes. Science. 2020:eabc1669.
24. Walls AC, Park Y-J, Tortorici MA, Wall A, McGuire AT, Veesler D. Structure, Function, and Antigenicity of the SARS-CoV-2 Spike Glycoprotein. Cell. 2020;181(2):281-92.e6.
25. Zheng M, Song L. Novel antibody epitopes dominate the antigenicity of spike glycoprotein in SARS-CoV-2 compared to SARS-CoV. Cellular & Molecular Immunology. 2020;17(5):536-8.
26. Stalin Raj V, Okba NMA, Gutierrez-Alvarez J, Drabek D, van Dieren B, Widagdo W, et al. Chimeric camel/human heavy-chain antibodies protect against MERS-CoV infection. Sci Adv. 2018;4(8):eaas9667.
27. Zhao G, He L, Sun S, Qiu H, Tai W, Chen J, et al. A Novel Nanobody Targeting Middle East Respiratory Syndrome Coronavirus (MERS-CoV) Receptor-Binding Domain Has Potent Cross-Neutralizing Activity and Protective Efficacy against MERS-CoV. J Virol. 2018;92(18).
28. Jiang S, Hillyer C, Du L. Neutralizing Antibodies against SARS-CoV-2 and Other Human Coronaviruses. Trends Immunol. 2020.
29. Flajnik MF, Kasahara M. Origin and evolution of the adaptive immune system: genetic events and selective pressures. Nat Rev Genet. 2010;11(1):47-59.
30. Muyldermans S. Nanobodies: natural single-domain antibodies. Annu Rev Biochem. 2013;82:775-97.
31. Cortez-Retamozo V, Backmann N, Senter PD, Wernery U, De Baetselier P, Muyldermans S, et al. Efficient cancer therapy with a nanobody-based conjugate. Cancer Res. 2004;64(8):2853-7.
32. Baral TN, Magez S, Stijlemans B, Conrath K, Vanhollebeke B, Pays E, et al. Experimental therapy of African trypanosomiasis with a nanobody-conjugated human trypanolytic factor. Nat Med. 2006;12(5):580-4.
33. Coppieters K, Dreier T, Silence K, de Haard H, Lauwereys M, Casteels P, et al. Formatted anti-tumor necrosis factor alpha VHH proteins derived from camelids show superior potency and targeting to inflamed joints in a murine model of collagen-induced arthritis. Arthritis Rheum. 2006;54(6):1856-66.
34. Arbabi Ghahroudi M, Desmyter A, Wyns L, Hamers R, Muyldermans S. Selection and identification of single domain antibody fragments from camel heavy-chain antibodies. FEBS Lett. 1997;414(3):521-6.
35. Dumoulin M, Conrath K, Van Meirhaeghe A, Meersman F, Heremans K, Frenken LG, et al. Single-domain antibody fragments with high conformational stability. Protein Sci. 2002;11(3):500-15.
36. Martsev SP, Chumanevich AA, Vlasov AP, Dubnovitsky AP, Tsybovsky YI, Deyev SM, et al. Antiferritin single-chain Fv fragment is a functional protein with properties of a partially structured state: comparison with the completely folded V(L) domain. Biochemistry. 2000;39(27):8047-57.

37. Romao E, Morales-Yanez F, Hu Y, Crauwels M, De Pauw P, Hassanzadeh GG, et al. Identification of Useful Nanobodies by Phage Display of Immune Single Domain Libraries Derived from Camelid Heavy Chain Antibodies. Curr Pharm Des. 2016;22(43):6500-18.
38. Fulcher LJ, Hutchinson LD, Macartney TJ, Turnbull C, Sapkota GP. Targeting endogenous proteins for degradation through the affinity-directed protein missile system. Open Biol. 2017;7(5).
39. Fulcher LJ, Macartney T, Bozatzi P, Hornberger A, Rojas-Fernandez A, Sapkota GP. An affinity-directed protein missile system for targeted proteolysis. Open Biol. 2016;6(10).
40. Ibrahim AFM, Shen L, Tatham MH, Dickerson D, Prescott AR, Abidi N, et al. Antibody RING-Mediated Destruction of Endogenous Proteins. Mol Cell. 2020.
41. Romao E, Poignavent V, Vincke C, Ritzenthaler C, Muyldermans S, Monsion B. Construction of High-Quality Camel Immune Antibody Libraries. Methods Mol Biol. 2018;1701:169-87.
42. Salema V, Fernandez LA. Escherichia coli surface display for the selection of nanobodies. Microb Biotechnol. 2017;10(6):1468-84.
43. Pinero-Lambea C, Bodelon G, Fernandez-Perianez R, Cuesta AM, Alvarez-Vallina L, Fernandez LA. Programming controlled adhesion of E. coli to target surfaces, cells, and tumors with synthetic adhesins. ACS Synth Biol. 2015;4(4):463-73.
44. Salema V, Manas C, Cerdan L, Pinero-Lambea C, Marin E, Roovers RC, et al. High affinity nanobodies against human epidermal growth factor receptor selected on cells by E. coli display. MAbs. 2016;8(7):1286-301.
45. Salema V, Marin E, Martinez-Arteaga R, Ruano-Gallego D, Fraile S, Margolles Y, et al. Selection of single domain antibodies from immune libraries displayed on the surface of E. coli cells with two beta-domains of opposite topologies. PLoS One. 2013;8(9):e75126.
46. Salema V, Lopez-Guajardo A, Gutierrez C, Mencia M, Fernandez LA. Characterization of nanobodies binding human fibrinogen selected by E. coli display. J Biotechnol. 2016;234:58-65.
47. David D, Rotenberg D, Khinich E, Erster O, Bardenstein S, van Straten M, et al. Middle East respiratory syndrome coronavirus specific antibodies in naturally exposed Israeli llamas, alpacas and camels. One Health. 2018;5:65-8.
48. Jin L, Cebra CK, Baker RJ, Mattson DE, Cohen SA, Alvarado DE, et al. Analysis of the genome sequence of an alpaca coronavirus. Virology. 2007;365(1):198-203.
49. Rodon J, Okba NMA, Te N, van Dieren B, Bosch BJ, Bensaid A, et al. Blocking transmission of Middle East respiratory syndrome coronavirus (MERS-CoV) in llamas by vaccination with a recombinant spike protein. Emerg Microbes Infect. 2019;8(1):1593-603.
50. Brown BL, McCullough J. Treatment for emerging viruses: Convalescent plasma and COVID-19. Transfus Apher Sci. 2020;59(3):102790.
51. Duan K, Liu B, Li C, Zhang H, Yu T, Qu J, et al. Effectiveness of convalescent plasma therapy in severe COVID-19 patients. Proc Natl Acad Sci U S A. 2020;117(17):9490-6.
52. Rojas M, Rodriguez Y, Monsalve DM, Acosta-Ampudia Y, Camacho B, Gallo JE, et al. Convalescent plasma in Covid-19: Possible mechanisms of action. Autoimmun Rev. 2020;19(7):102554.
53. Wrapp D, De Vlieger D, Corbett KS, Torres GM, Wang N, Van Breedam W, et al. Structural Basis for Potent Neutralization of Betacoronaviruses by Single-Domain Camelid Antibodies. Cell. 2020;181(5):1004-15 e15.
54. Hanke L, Perez LV, Sheward DJ, Das H, Schulte T, Morro AM, et al. An alpaca nanobody neutralizes SARS-CoV-2 by blocking receptor interaction. bioRxiv. 2020:2020.06.02.130161.
55. Els Conrath K, Lauwereys M, Wyns L, Muyldermans S. Camel single-domain antibodies as modular building units in bispecific and bivalent antibody constructs. J Biol Chem. 2001;276(10):7346-50.

56. Conrath KE, Lauwereys M, Galleni M, Matagne A, Frere JM, Kinne J, et al. Beta-lactamase inhibitors derived from single-domain antibody fragments elicited in the camelidae. Antimicrob Agents Chemother. 2001;45(10):2807-12.

Figure- 1

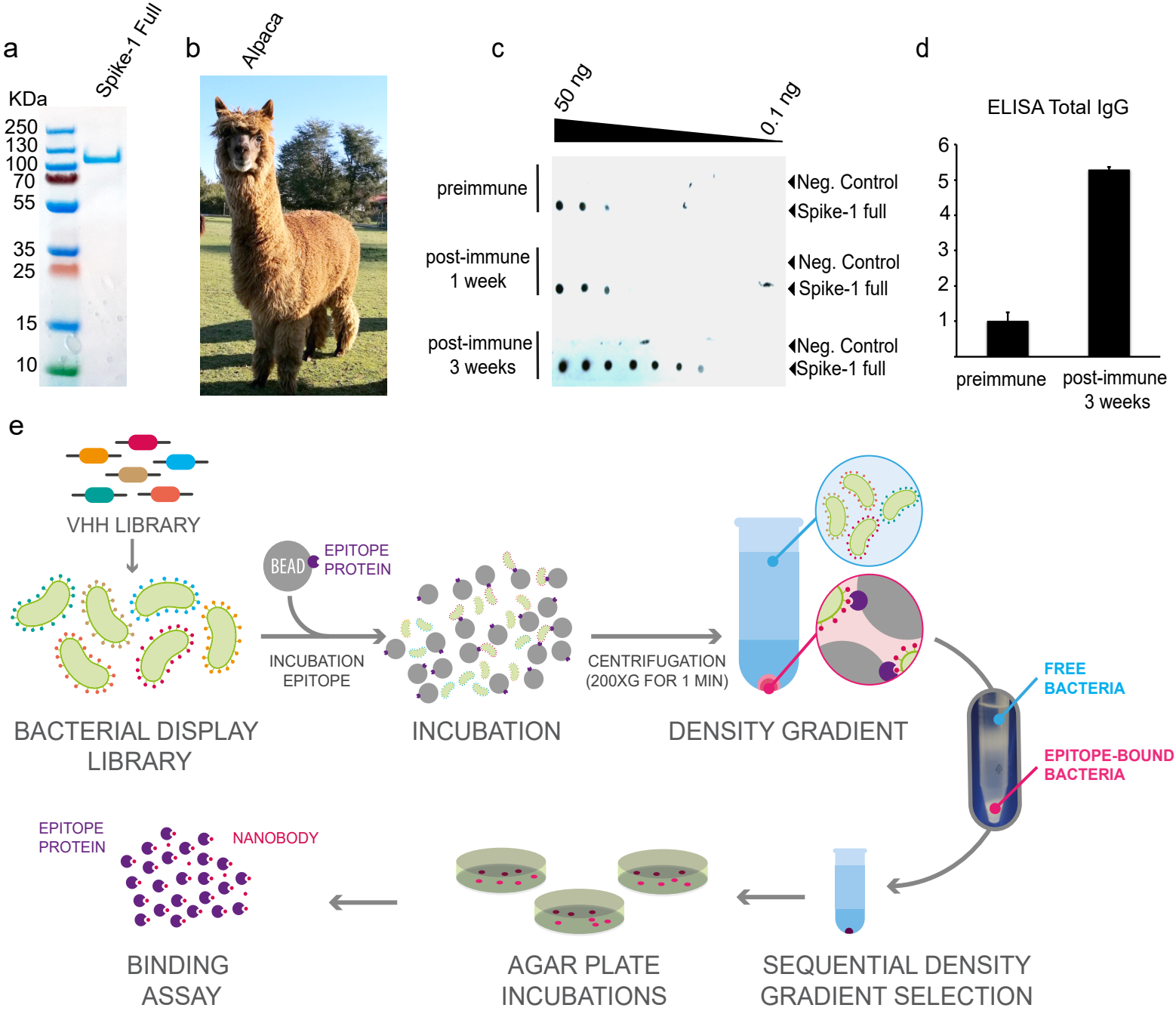
a
Spike-1 Full
KDa
250
130
100
70
55
35
25
15
10
b
Alpaca
c
50 ng
0.1 ng
preimmune
post-immune 1 week
post-immune 3 weeks
Neg. Control
Spike-1 full
Neg. Control
Spike-1 full
Neg. Control
Spike-1 full
d
ELISA Total IgG
6
5
4
3
2
1
preimmune
post-immune 3 weeks
e
VHH LIBRARY
BACTERIAL DISPLAY LIBRARY
BEAD
EPITOPE PROTEIN
INCUBATION EPITOPE
INCUBATION
CENTRIFUGATION (200XG FOR 1 MIN)
DENSITY GRADIENT
FREE BACTERIA
EPITOPE-BOUND BACTERIA
SEQUENTIAL DENSITY GRADIENT SELECTION
AGAR PLATE INCUBATIONS
EPITOPE PROTEIN
NANOBODY
BINDING ASSAY

Figure- 2

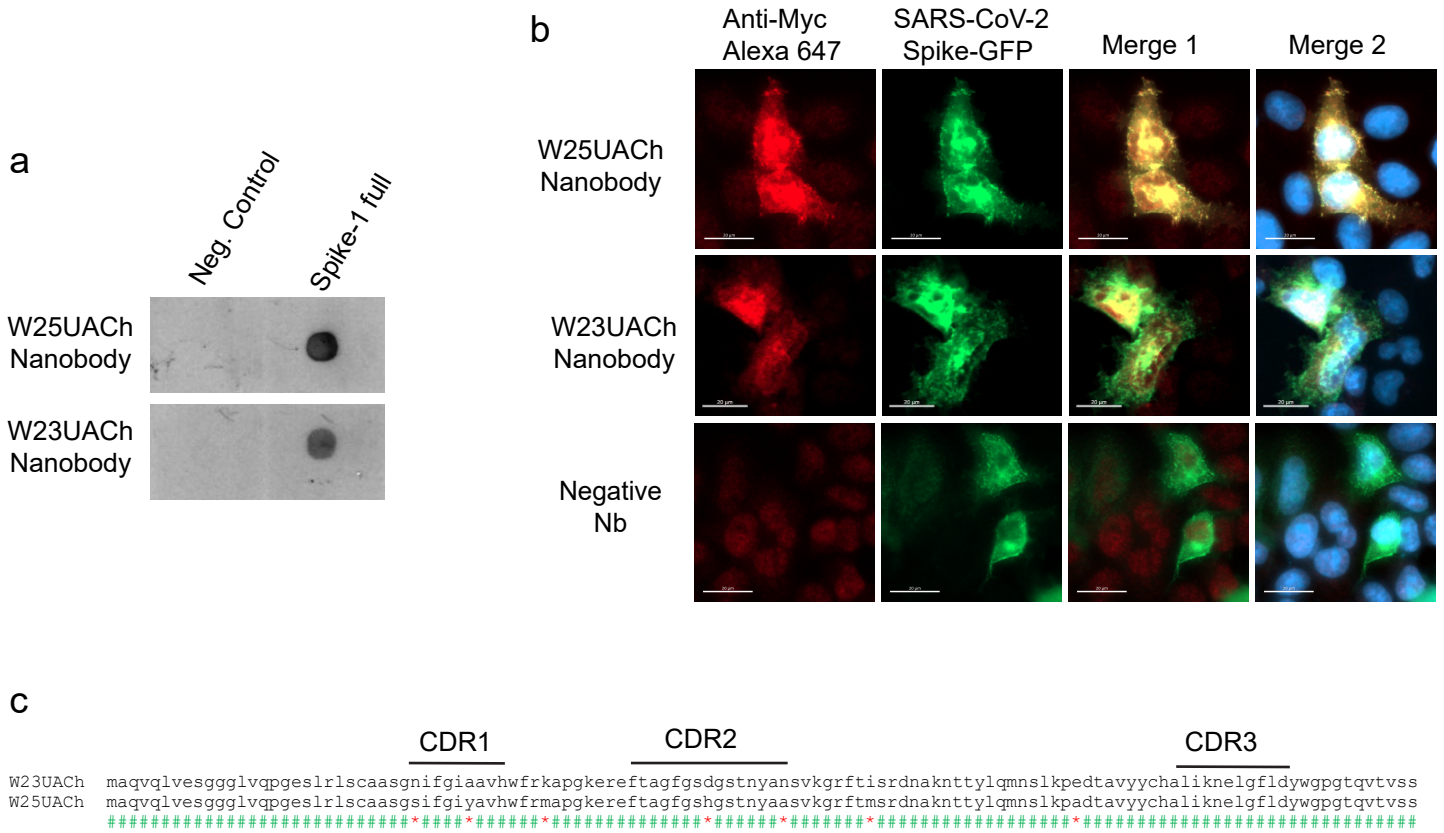
a
Neg. Control
Spike-1 full
W25UACh Nanobody
W23UACh Nanobody
b
Anti-Myc Alexa 647
SARS-CoV-2 Spike-GFP
Merge 1
Merge 2
W25UACh Nanobody
W23UACh Nanobody
Negative Nb
c
CDR1
CDR2
CDR3
W23UACh maqvqlvesggglvqpgeslrlscaasgnifgiaavhwfrkapgkereftagfgsdgstnyansvkgrftisrdnaknttylqmnslkpedtavyychaliknelgfldywgpgtqvtvss
W25UACh maqvqlvesggglvqpgeslrlscaasgsifgiyavhwfrmapgkereftagfgshgstnyaasvkgrftmsrdnaknttylqmnslkpadtavyychaliknelgfldywgpgtqvtvss
##########################*####*######*##############*######*#######*##################*##############################

Figure- 3

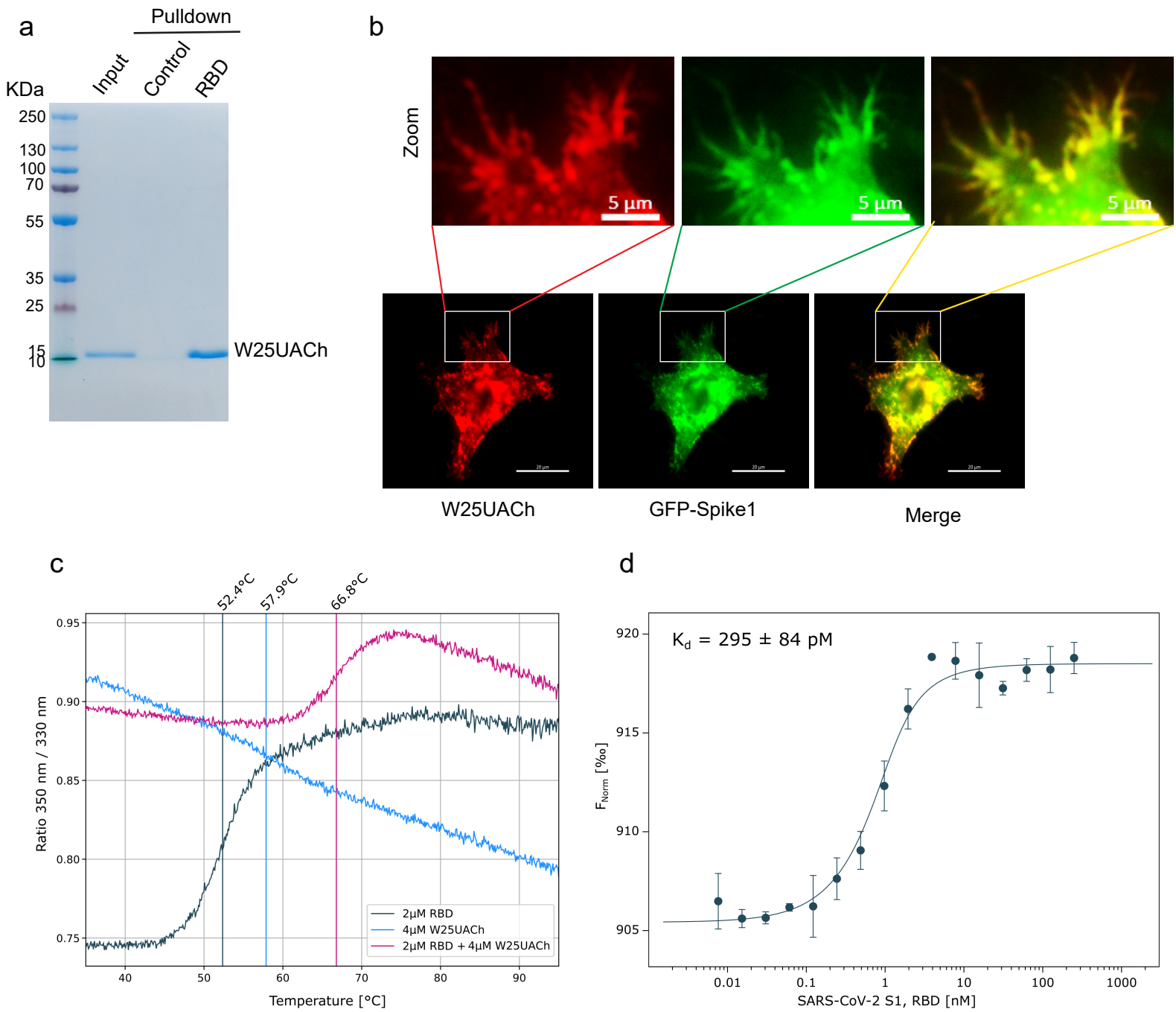
a
Pulldown
Input
Control
RBD
KDa
250
130
100
70
55
35
25
15
10
W25UACh
b
Zoom
5 µm
5 µm
5 µm
W25UACh
GFP-Spike1
Merge
c
52.4°C
57.9°C
66.8°C
Ratio 350 nm / 330 nm
Temperature [°C]
2µM RBD
4µM W25UACh
2µM RBD + 4µM W25UACh
d
K_d = 295 ± 84 pM
F_{Norm} [‰]
SARS-CoV-2 S1, RBD [nM]